RHIC LUMINOSITY INCREASE WITH BUNCHED BEAM STOCHASTIC COOLING*

M. Blaskiewicz[†], J.M. Brennan, K. Mernick
BNL, Upton, NY, 11973, USA

Abstract

The RHIC luminosity increase with bunched beam stochastic cooling is reviewed. Most notably, during 2012 with uranium beams, we observed a tripling of instantaneous luminosity and a 5 fold increase in integrated luminosity.

INTRODUCTION

A stochastic cooling system is a wide band feedback loop [1, 2]. A pickup detects fluctuations in the beam current or transverse position. This signal is filtered, amplified and sent to a kicker. When the system is correctly adjusted the perturbations created by the kicker reduce the detected signal. Over time this acts as a viscous force causing the beam to condense or cool. The fundamentals are illustrated in Figure 1. The Schottky current from the beam I_S is detected by the pickup P. There is also a signal associated with the coherent response of the beam due to the kicker, I_1. The sum of these currents is filtered and amplified through an effective transfer impedance, Z_T. A voltage, $V_K = -Z_T(I_S + I_1)$ is generated by the kicker. For appropriate phases and gains the beam is cooled, resulting in a small change to the Schottky signal. In addition to the desired change to the Schottky signal there is a much larger coherent response due to the beam transfer function, $I_1 = BV_K$. The beam transfer function depends on the beam properties in the fluid limit and evolves slowly over a cooling time. Over time scales short compared to the cooling time one may neglect the slow evolution of B and directly relate the kicker voltage to the Schottky current,

$$V_K = \frac{-Z_T I_S}{1 + BZ_T}. \tag{1}$$

Some additional calculation yields

$$I_{total} = I_1 + I_S = \frac{I_S}{1 + BZ_T}. \tag{2}$$

The second result demonstrates signal suppression or shielding [3]. The total current, I_{total} is directly measurable. The transfer impedance is adjusted to give $I_{total} \approx I_S/2$ and I_S measured with feedback off. With system bandwidth W one obtains a time resolution $\tau \sim 1/2W$. For a beam of particles with charge q and current I, the longitudinal cooling system measures the average energy of samples containing $N_s = I\tau/q$ particles each turn. This

Figure 1: Schematic of the cooling feedback loop.

signal is filtered, amplified and applied to the beam so as to reduce the energy spread. If the beam requires M turns to mix the samples into statistical independence, the optimal cooling time scales as $\sigma_E/\dot{\sigma}_E \approx 2N_sT_0M$ where the revolution period is $T_0 = 12.8\mu$s for RHIC.

The RHIC system has greatly benefitted from previous work. Bunched beam stochastic cooling was first observed in 1978 in ICE [4]. In the initial publication it was noted that correlated synchrotron sidebands imply that the optimal cooling gain need not be flat in frequency, as in the coasting beam case, but could have maxima spaced at the inverse of the bunch length. The RHIC system exploits this property.

A theory of bunched beam cooling was developed in the early eighties [5, 6, 7, 8] and stochastic cooling systems for the SPS [7, 9] and the Tevatron [7, 10] were explored. Stochastic cooling in RHIC was first studied by Van de Meer [11] and extended by Wei and Ruggerio [12, 13]. Experimental studies for the SPS and the Tevatron were started and early on [10, 14, 15, 16, 17] it was found that "RF activity" extending up to very high frequencies dwarfed the true Schottky signal. Nonetheless, stochastic cooling work in the Tevatron continued. Promising results were obtained but not pursued [18].

Experimental studies in RHIC began in 2002 with measurements of gold Schottky spectra and preliminary calculations [19]. In 2003 longitudinal beam transfer functions were presented and quantitative agreement of kicker voltage with beam response was obtained [20]. In 2004 the longitudinal kicker voltage was estimated at several kilovolts [21], similar to earlier estimates[11]. Around the same time the notion of using narrow band cavities and a Fourier series implementation was introduced [22]. The

narrow band approach allowed for multi-kilovolt kicks with modest equipment. It is fair to say that this technique is needed for practical stochastic cooling in RHIC.

In 2005 preliminary results for longitudinal cooling in RHIC were presented [23]. Signal suppression was demonstrated and the technique of using two, one turn delay filters in series was introduced. In 2006 we saw longitudinal cooling using a low intensity proton bunch [24]. An algorithm to do accurate simulations was developed and the results compared well with data [25]. A critical finding of the simulations was that the migration of longitudinal action, due the the combined effects of intrabeam scattering (IBS) and cooling, was very beneficial to transverse cooling. In 2007 longitudinal cooling was made operational [26, 27]. We continued working on the systems [28] and achieved three dimensional cooling in 2010 [29]. We had a vertical cooling system and used betatron coupling to cool the horizontal emittance. Horizontal cooling systems were operational in 2012 and used to great effect in uranium-uranium and copper-gold collisions [30].

RHIC STOCHASTIC COOLING SYSTEM

The RHIC stochastic cooling system layout is shown in Figure 2 and relevant parameters are shown in Table 1. We use one turn delay filter cooling [31] for the longitudinal system. Both rings are similar so we will discuss the blue (clockwise) ring. The pickup is in the 2 o'clock straight section. This pickup signal is processed through a 16 branch traversal filter giving

$$V_t(t) = \sum_{n=0}^{15} V_p(t - n\tau_0), \qquad (3)$$

with $\tau_0 = 5.000$ ns. The filter is constructed from coaxial cables, without active components that could saturate. The signal is amplified and sent to the 4 o'clock receiver using an analog, 70 GHz microwave link [32] resulting in a pickup to kicker delay of 1/6th of a turn. The signal then goes through a one turn delay filter constructed from single mode optical fiber. A key feature is that the modulation of the optical signal is accomplished via attenuation of the laser source, which reduces nonlinear effects. After the one turn delay filter the signal is split into 16 branches and the signals are passed through 100 MHz bandpass filters centered at $6.0, 6.2, \ldots, 9.0$ GHz. These signals go through IQ modulators and then to 40 W solid state amplifiers that power individual cavities. The cavities are split along the vertical plane and are open during injection and acceleration. After reaching top energy they close down to a 2cm aperture.

The transverse cooling system pickup plates were provided by FNAL [33] and are moved with $5\mu m$ precision translation stages. A difference signal is obtained and a 16 stage traversal filter is a applied. To avoid crosstalk the yellow (counterclockwise) ring uses frequencies $4.8, 5.0, \ldots 7.8$ GHz while the blue ring uses $4.7, 4.9, \ldots 7.7$ GHz. The latter is obtained by inserting
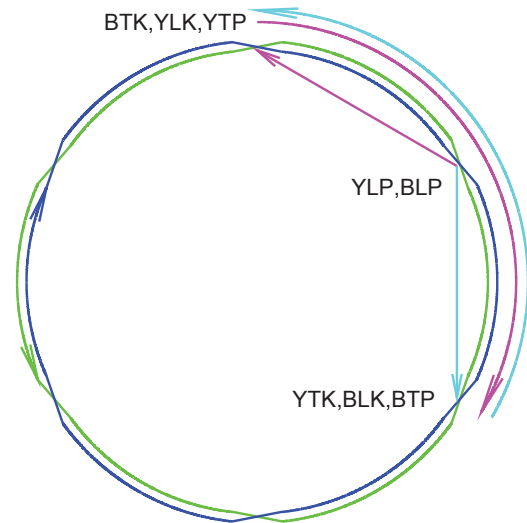
Figure 2: Schematic of the blue (clockwise) and yellow (counterclockwise) RHIC rings showing the locations of stochastic cooling components. The blue transverse kickers (BTK),yellow longitudinal kicker (YLK) and yellow transverse pickups (YTP) are in the 12 o'clock straight sections. The blue and yellow longitudinal pickups (BLP,YLP) are in the 2 o'clock straight sections. The yellow transverse kickers (YTK),blue longitudinal kicker (BLK) and blue transverse pickups (BTP) are in the 4 o'clock straight sections. The tellow beam path is green, with signal paths in magenta. The blue beam path is dark blue, with signal paths in light blue.

Table 1: RHIC Parameters During the 2011 Uranium Run

Parameter	Value
circumference	3834 m
betatron tunes	$Q_{x,y} = 28.22, 29.22$
transition gamma	25.22
beam energy	103.5 GeV/nucleon
ions/bunch	2.3×10^8
h=2520 voltage	2.8 MV
h=360 voltage	0.30 MV
inital 95% emittance	$14\pi \, \mathrm{mm} - \mathrm{mrad(normalized)}$

a -1^n in (3). The signals are sent to their kickers via optical fiber for a net delay of 2/3rd of a turn. The kicker cavities are similar to the longitudinal cavities except that we couple to a transverse mode via offset of the coupler.

During operation the 96 independent cavity systems are computer controlled. One cavity at a time, transfer switches insert a network analyzer in the signal path. The open loop transfer function is measured and compared to a reference that had good cooling. The IQ modulators are adjusted to make the live transfer function as close to the stored as possible. In this way we step though all the cavities at startup and about every 15 minutes hence, to accommodate system drifts and changes in the beam.

SIMULATIONS AND COMPARISON WITH DATA

The simulation algorithm relies on the fact that stochastic cooling times are proportional to the number of particle in a sample. A thought experiment will illustrate the main points. Consider an actual beam with $N \sim 10^9$ ions. The actual value of N is irrelevant as long as it is big enough to preclude direct simulation. Next imagine some binding force causes the ions to bind together in groups of R. The new beam will have N/R ions but the same beam current, rigidity, transverse emittance and other fluid limit properties as the original beam. However, for fixed gain (no saturation!), the signal power from a stochastic cooling pickup will be a factor R larger for the second beam and the optimal cooling rate will be a factor R bigger. Details of the cooling implementation can be found in [34] with the caveats that transverse cooling systems for both planes are now included and the longitudinal cooling system now uses only a single one turn delay filter. Reference [34] also detailed our implementation of intrabeam scattering. Currently, we use IBS kicks in all 3 dimensions and provide betatron coupling via a skew quadrupole.

The final part of the simulations involves the effect of particle loss due to burn-off from collisions. The spatial density for a round, relativistic beam traveling in the negative z direction is

$$n(x, y, z, t) = \frac{I(t + z/c)e^{-(x^2 + y^2)/2\epsilon\beta(z)}}{2\pi q c \epsilon \beta(z)}, \quad (4)$$

where $\beta(z) = \beta_* + z^2/\beta_*$ is the beta function, $I(t)$ is the current across the interaction plane (IP), and ϵ is the unnormalized rms emittance. Consider a particle traveling in the positive z direction with $x(z) = x_0 + \theta_x z$, $y(z) = y_0 + \theta_y z$, $z = c(t - t_0)$. The probability this particle interacts with the oncoming beam is

$$P = 2\sigma \int n(x(z), y(z), z, t_0 + z/c) dz, \quad (5)$$

where σ is the cross section and we have ignored fractional corrections of order θ_x^2. To reduce noise and computation time we average (5) over the betatron phases giving

$$P = F(\alpha_x)F(\alpha_y)\sigma \int dz \frac{I(t_0 + 2z/c)}{\pi q c \epsilon \beta(z)}, \quad (6)$$

where

$$\alpha_x = \frac{x_0^2 + \beta_*^2 \theta_x^2}{4\beta^* \epsilon}$$

and $F(\alpha) = \exp(-\alpha)I_0(\alpha)$. The parameters $\alpha_{x,y}$ depend only on the particle's emittance so no special transport through the IP needs to be calculated. The integral in (6) is calculated on a grid in t_0 and the values of F are calculated for each particle.

Equation (6) gives the probability that one of the particles in the actual beam is burned off during a single passage through the IP. The simulations are accelerated by a factor of R so equation (6) needs multiplication by this same factor. Interestingly, the average number of simulation particles lost per turn is the same as the average number of actual particles lost per turn. We go on to report experimental results and compare them with simulations

The RHIC system with horizontal cooling has been used during uranium-uranium and copper-gold runs. The copper-gold run was complicated by differing cooling rates and beam-beam effects so we consider uranium-uranium running.
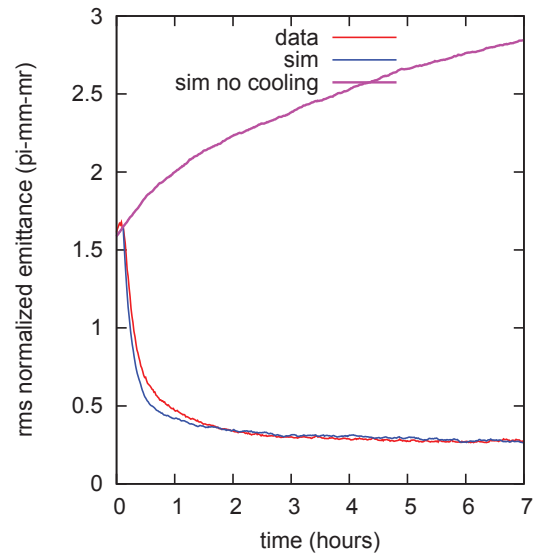
Figure 3: Evolution of rms emittance.
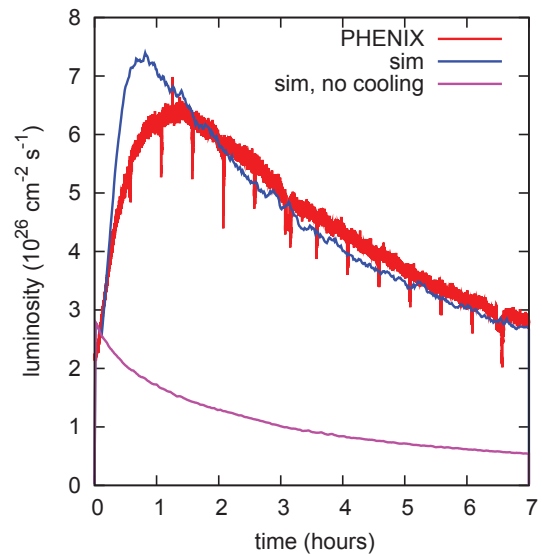
Figure 4: Luminosity versus time.

Figure 3 shows the time evolution of the rms nomalized emittance for data and simulation, a simulation with the
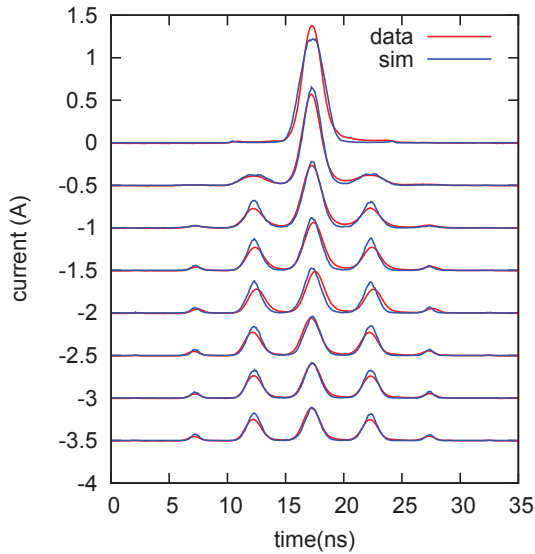
Figure 5: Evolution of beam current,
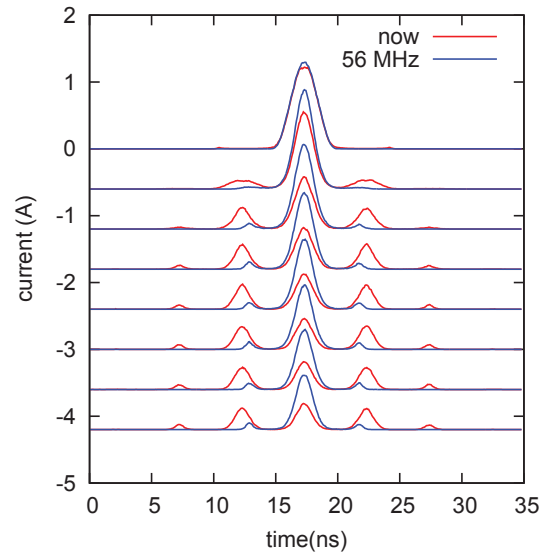
Figure 7: Effect of 56 MHz cavity on beam current.
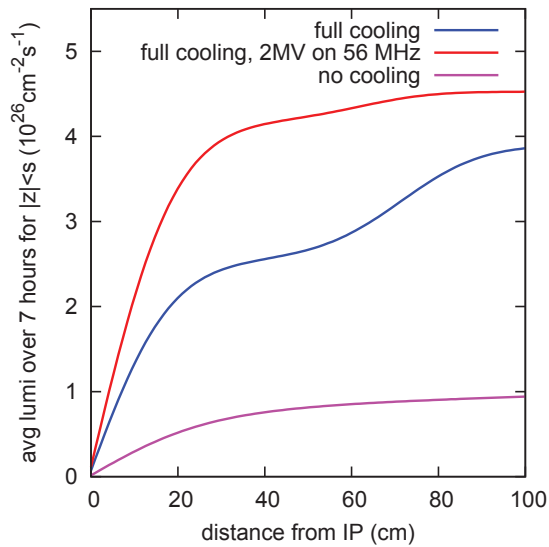
Figure 6: Luminosity versus vertex and effect of 56 MHz cavity.

Figure 8: Effect of cooling on luminosity.

same inital conditions but no cooling is shown for comparison. The asymptotic value of $0.27 mm - mrad$ in the cooled beam is exceptionally small, leading to significant luminosity improvement as shown in Fig. 4. The evolution of the longitudinal profiles is shown in Fig. 5. While we clearly lose beam from the cental bucket the rate is far smaller than without longitudinal cooling. Figure 6 shows the average luminosity as a function of vertex cut for nominal cooling, cooling with the addition of a 56 MHz cavity at 2 MV [36] and with no cooling. The benefits of current and planned upgrades are fairly clear. Longitudinal profiles with and without the 56 MHz cavity are illustrated in Fig. 7. The improved longitudinal confinement with the 56 MHz cavity significantly reduces longitudinal growth leading to enhanced luminosity, particularly for small vertex cuts.

We close this section with the experimental data in Fig. 8. When compared with no cooling, cooling in all 3 dimensions increases the instaneous luminosity by a factor of 3 and the integrated luminosity is increased by a factor of 5.

UPGRADES

We are in the process of upgrading both pickups and kickers for the longitudinal cooling systems. For the pickups we have implemented a new "keyhole" design, shown in Fig. 9. During injection and acceleration the beam is near the center of the large round chamber. After reaching top energy we use bellows to move the chamber so the
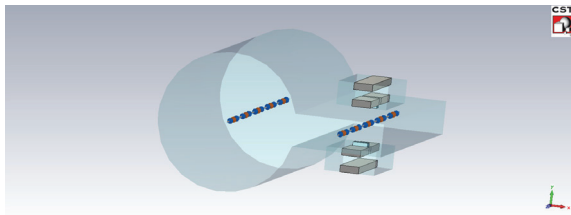
Figure 9: Key hole longitudinal pickup.
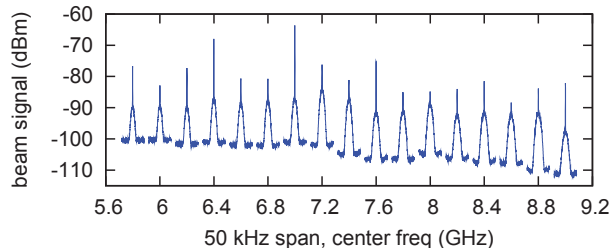
Figure 10: Beam spectra using the key hole longitudinal pickup. Each trace has a bandwidth of 50 kHz. The traces are centered at $5.8, 6.0, \ldots 9.0$ GHz.

beam is in the notch on the right. Reducing the aperture cuts off all propagating waves below 9 GHz. In addition to this note that the two waveguide ports do not have the same position along the beam direction. With this configuration the pickup gain as a function of frequency is much flatter than when the ports have the same longitudinal position.

For the kickers we are going from 4 to 6 cell cavities, which should increase our voltage by a factor of $\sqrt{6/4} = 1.22$. In addition to this we are coupling energy into the cavity via a waveguide as opposed to a coaxial cable, eliminating coaxial cables within the vacuum chamber.

ACKNOWLEDGMENTS

REFERENCES

[1] S. Van de Meer, *Rev. Mod. Phys* **57**, No. 3, part 1, p689 (1985).

[2] D. Mohl, CERN 87-03, p 453 (1987).

[3] F. Sacherer CERN-ISR-TH/78-11 (1978).

[4] H. Herr, D. Mohl, Porc. Workshop on Phase Space Cooling of High Energy Beams, Madison WI, USA, 1978. also, CERN/EP/Note 79-34 (1979), and CERN/PS/DL/Note 79-3 (1979).

[5] S. Chattopadhyay, LBL-14826, (1982).

[6] S. Chattopadhyay, IEEE TNS **30**, No. 4, p2646, 1983.

[7] S. Chattopadhyay, IEEE TNS **30**, No. 4, p2334, 1983.

[8] S. Chattopadhyay, IEEE TNS **30**, No. 4, p2649, 1983.

[9] D. Boussard, S. Chattopadhyay, G. Dome, T. Linnecar, CERN 84-15, p197, (1984).

[10] G. Jackson, PAC91, p2532, 1991.

[11] S. Van de Meer, RHIC-AP-9 (1984).

[12] J. Wei, A.G. Ruggiero, BNL/AD/RHIC-71 (1990).

[13] J. Wei, Workshop on Beam Cooling, Montreux, 1993, CERN 94-03, (1994).

[14] D. Boussard, Proc. Joint US-CERN Acc. School, Texas, 1986, Lecture Notes on Phys. 296, p289

[15] G. Jackson, J. Marriner, D. McGinnis, R. Pasquinelli, D. Peterson, Workshop on Advanced Beam Instrumentation, Tsukuba, p312, (1991).

[16] F. Caspers, D. Mohl, XVII International Conference on High Energy Accelerators, Dubna, Russia, (1998). also CERN/PS 98-051 (DI).

[17] G. Jackson, Workshop on Beam Cooling, Montreux, 1993, CERN 94-03, (1994).

[18] R.J. Pasquinelli, Proccedings of the 1995 Particle Accelerator Conference, p2379 (1995).

[19] J.M. Brennan, M. Blaskiewicz, P. Cameron, J. Wei, 308, EPAC02

[20] M. Blaskiewicz, J.M. Brennan, P. Cameron, J. Wei, PAC03, p394.

[21] J. Wei, M. Blaskiewicz, J.M. Brennan EPAC04, p941, (2004).

[22] M. Blaskiewicz, J.M. Brennan, J. Wei, EPAC04, p2861, (2004).

[23] M. Blaskiewicz, PAC05, p310, (2005).

[24] J.M. Brennan, M. Blaskiewicz, F. Severino EPAC06.

[25] M. Blaskiewicz, J.M. Brennan *Phys. Rev. ST Accel. Beams* 061001, (2007).

[26] M. Blaskiewicz, J.M. Brennan, F.Severino, Proccedings of the 2007 Particle Accelerator Conference, p2014 (2007).

[27] M. Blaskiewicz, J.M. Brennan, F. Severino, *Phys. Rev. Lett.* **100** 174802 (2008).

[28] J.M. Brennan, M. Blaskiewicz, PAC09, p1910 (2009).

[29] M. Blaskiewicz, J.M. Brennan, K. Mernick, *Phys. Rev. Lett.* **105** 094801 (2010).

[30] J.M. Brennan, M. Blaskiewicz, K.Mernick, IPAC2012, p2900, WEPPP082, (2012)

[31] G. Carron, L. Thorndahl CERN-ISR-RF/78-12 (1978).

[32] K. Mernick, M. Blaskiewica, J.M. Brennan, B. Johnson, F. Severino, BIW10, p389, TUPSM085, (2010).

[33] D. McGinnis, J. Budlong, G. Jackson, J. Marriner, D. Poll, PAC01, p1389 (1991).

[34] M.Blaskiewicz, J.M. Brennan, COOL07 (2007)

[35] see *e.g.* pg 126 in 'Handbook of Accelerator Physics and Engineering', A. Chao, M. Tigner *eds.* World Scientific, 1999.

[36] A.V. Fedotov, I. Ben-Zvi, WE6PFP004 PAC09 P2483 (2009).